Ignition Characteristics of Heptane-Hydrogen and Heptane-Methane Fuel Blends at Elevated Pressures

S. K. Aggarwal, O. Awomolo, K. Akber
Department of Mechanical and Industrial Engineering
University of Illinois at Chicago, IL 60607

Submitted to International Journal of Hydrogen Energy
(Revised on August 15, 2011)

Corresponding Author: S. K. Aggarwal
University of Illinois at Chicago,
842 W. Taylor St, Chicago, IL 60607, USA
Phone: 312-996-2235
Fax: 312-413-0447
ska@uic.edu

ABSTRACT

There is significant interest in using hydrogen and natural gas for enhancing the performance of diesel engines. We report herein a numerical investigation on the ignition of n-C_7H_{16}/H_2 and n-C_7H_{16}/CH_4 fuel blends. The CHEMKIN 4.1 software is used to model ignition in a closed homogenous reactor under conditions relevant to diesel/HCCI engines. Three reaction mechanisms used are (i) NIST mechanism involving 203 species and 1463 reactions, (ii) Dryer mechanism with 116 species and 754 reactions, and (iii) a reduced mechanism (Chalmers) with 42 species and 168 reactions. The parameters include pressures of 30atm and 55atm, equivalence ratios of ϕ=0.5, 1.0 and 2.0, temperature range of 800-1400K, and mole fractions of H_2 or CH_4 in the blend between 0-100%. For n-C_7H_{16}/air mixtures, the Chalmers mechanism not only provides closer agreement with measurements compared to the other two mechanisms, but also reproduces the negative temperature coefficient regime. Consequently, this mechanism is used to characterize the effects of H_2 or CH_4 on the ignition of n-C_7H_{16}. Results indicate that H_2 or CH_4 addition has a relatively small effect on the ignition of n-C_7H_{16}/air mixtures, while the n-C_7H_{16} addition even in small amount modifies the ignition of H_2/air and CH_4/air mixtures significantly. The n-C_7H_{16} addition decreases and increases the ignition delays of H_2/air mixtures at low and high temperatures, respectively, while its addition to CH_4/air mixtures decreases ignition delays at all temperatures. The sensitivity analysis indicates that ignition characteristics of these fuel blends are dominated by the pyrolysis/oxidation chemistry of n-heptane, with heptyl (C_7H_{16}-2) and hydoxyl (OH) radicals being the two most important species.

1. Introduction

There is worldwide interest in the use of renewable and environmentally fuels for transportation and power generation. This is being driven by our concerns for greenhouse gas emissions, climate change, and dwindling supplies of fossil fuels. In this regard, both hydrogen and natural gas can play a major role in addressing these concerns, and help us move towards a carbon neutral economy. Hydrogen is known to have significant advantage over conventional fossil fuels in terms of combustion efficiency and emissions. For instance, hydrogen provides greater energy release per unit mass (about 2.6 times that of gasoline), and reduces green house gas and particulate emissions significantly. It also has superior ignition characteristics and much wider flammability limits compared to hydrocarbon fuels. Moreover, it can be produced from a number of sources and provide significant flexibility in harnessing its energy through a variety of technologies, including hydrogen powered internal combustion engines (H_2-ICE), fuel cells (H_2-FC), hybrid systems (H_2-ICE/H_2-FC and H_2-ICE/battery combinations), and H_2 blended with other fuels [1]. However, H_2 being an energy carrier, i.e., not a direct source of energy, presents many challenges associated with its production and storage, especially due to its low ignition energy, and low volumetric energy content. There are also unresolved issues with regards to H_2 combustion, such as knock, detonation, flame stability, and flashback. In this context, hydrogen-hydrocarbon fuel blends offer a promising alternative, as they can synergistically resolve the storage and combustion problems associated with hydrogen and the emission problems associated with fossil fuel combustion. Consequently, there is considerable interest in investigating the ignition, combustion and emission characteristics of hydrogen-fossil fuel blends. Similarly, natural gas represents a significantly cleaner and low cost alternative to gasoline and diesel fuels. It is also increasingly becoming the fuel of choice for power generation. Consequently, several studies have examined the use of natural gas, both in the pure and blended form, in liquid-fueled combustion systems [2, 3, 4, 5].

Previous studies dealing with the combustion of hydrogen-hydrocarbon mixtures have mostly considered CH_4/H_2 blends. Both fundamental and practical aspects of using such blends for transportation and power generation have been investigated. Fundamental studies have focused on the effect of hydrogen addition on flammability limits [6], laminar [7,8] and turbulent [9] burning velocities, flame propagation characteristics including flame speed-

stretch interactions and Markstein length [8,10], flame stability [11], NOx emissions [6,12,13,14], and lean blowout limits [15,16] of methane flames. Different flame configurations, including laminar premixed [7,8], nonpremixed [14] and partially premixed flames [10,12], as well as burner stabilized [17,18] and swirl-stabilized [15,19] turbulent flames have been employed. In addition, there have been engine studies using blends of hydrogen with natural gas and other fuels [20,21]. The ignition characteristics of hydrogen-enriched methane-air mixtures have also been investigated. Levinsky et al. [22] studied the autoignition of stoichiometric methane-hydrogen mixtures in a rapid compression machine for pressure range of 15-70 atm and temperature range of 950-1060K, while Huang et al. [23] reported shock-tube ignition data for pressure range of 16- 50 atm and temperature range of 1000-1300K. Fotache et al. [24] reported an experimental-numerical investigation on the effect of hydrogen on methane ignition in a counterflow diffusion flame, and identified three ignition regimes, namely, hydrogen-assisted, transition, and hydrogen-dominated, based on the H_2 concentration. Safta and Madnia [25] numerically studied the ignition and flame evolution of hydrogen-enriched methane mixtures in a vortex ring. Ju and Niioka [26] performed a numerical study of the ignition of CH_4/H_2 mixtures in a supersonic mixing layer, and observed that the ignition enhancement is proportional to the amount of hydrogen in the blend.

Compared to CH_4/H_2 blends, studies dealing with n-C_7H_{16}/H_2 blends have been rather sparse, although the ignition and combustion characteristics of n-C_7H_{16} have been extensively investigated. Herzler et al. [27] and Gauthier et al. [28] reported shock tube ignition data for n-heptane/air mixtures at diesel and HCCI engine relevant conditions. There have also been a number of n-C_7H_{16} flame studies in counterflow [13, 29, 30, 31] and coflow configurations [32]. Since n-heptane is one of the reference fuels, and a surrogate for diesel fuel, its oxidation chemistry has been extensively investigated, and a number of detailed and skeleton mechanisms have been developed. These include (i) NIST mechanism [33], (ii) San Diego mechanism [34], (iii) Lawrence Livermore National Laboratory (LLNL) mechanism [35, 36], (iv) Dryer mechanism [37], (v) Ranzi mechanism [38], and (vi) a skeleton mechanism developed at the Chalmers University [39]. Our literature review indicated numerous studies on the ignition and combustion behavior n-heptane, but not on its blends with other fuels, especially with H_2 and CH_4. With regards to ignition, the literature contained two studies, one

dealing with n-C_7H_{16}/H_2 and n-C_7H_{16}/CO blends [40], and the other using n-C_7H_{16}/H_2 and n-C_7H_{16}/CH_4 blends [41].

This paper reports a numerical investigation on the ignition of n-C_7H_{16}/H_2 and n-C_7H_{16}/CH_4 blends at conditions relevant to diesel and HCCI engines. The selection of H_2 and CH_4 fuels is based on the consideration that there is significant interest in using hydrogen or natural gas to improve the performance of diesel engines, especially through a dual-fuel mode [42]. The focus of this study is on ignition under homogeneous, quiescent conditions so as to isolate chemical kinetics from fluid dynamics effects. Ignition delay data for n-heptane-air, hydrogen-air, and methane-air mixtures are used to validate several reaction mechanisms for these mixtures. Based on this comparison, the Chalmers mechanism is used for a detailed numerical study to examine the effects of H_2 and CH_4 on the ignition of n-C_7H_{16}/air mixtures at engine relevant conditions in terms of temperature, pressure, and equivalence ratio. Our interest in investigating the ignition behavior of these blends using the Chalmers mechanism also stems from the fact in a future study we plan to examine their combustion and emission characteristics in diesel engines. The paper is organized in the following manner. The physical-numerical model is briefly described in Section 2. Results of validation studies using different kinetic mechanisms are also presented in this section. Results characterizing the effects of H_2 and CH_4 on the ignition of n-C_7H_{16}/air mixtures, and also on the effect of n-C_7H_{16} on the ignition of H_2/air and CH_4/air mixtures are discussed in Section 3. Results of a sensitivity study to identify the dominant reactions associated with the ignition of these fuel blends are also presented in this section, followed by conclusions in the last section.

2. Physical-Numerical Model

The physical model is based on the transient, spatially homogeneous form of the conservation equations for mass, energy, and species in a given adiabatic system. Simulations were performed using the closed homogenous batch reactor model in CHEMKIN 4.1. The stiff set of equations is solved using an implicit time integration schemes as described in Ref. [43]. Computations are started with specified initial conditions, which include the initial temperature, pressure, and reactant mixture composition. As the exothermic reactions are initiated and the mixture temperature increases, the concentrations of radical species increase. Consequently, the chemical activity is accelerated and the rate of temperature increase is

enhanced. The state of ignition was defined when the mixture temperature increases by 400K over one time step during simulations. Using other ignition criteria, such as one based on OH radical mole fraction, yielded essentially the same ignition delay time. For validation, the ignition delay times computed using three different mechanisms were compared with the shock tube ignition data for n-heptane-air mixtures. The mechanisms include (i) the NIST mechanism [33] consisting of 203 species and 1463 reactions, (ii) the Dryer mechanism [37] with 116 species and 754 reactions and (iii) a reduced mechanism developed at Chalmers University [39], which is termed here as the Chalmers mechanism, consisting of 42 species and 168 reactions. Some results for the ignition of n-C_7H_{16}/H_2 blends using the LLNL (Lawrence Livermore National Laboratory) mechanism [44] are also presented. This is a more detailed mechanism with 654 species and 2827 reactions, and has been extensively validated for several hydrocarbon fuels including n-heptane.

Figure 1 represents a comparison of the predicted ignition delays, using the three mechanisms, with the experimental data of Gauthier et al. [28] for n-C_7H_{16}–air mixtures at equivalence ratio ϕ=1, and pressures of 13 and 55 atm. While all three mechanisms show discrepancies with respect to measurements, especially at high temperature and pressure, the NIST mechanism seems to perform better at 13atm, while the Chalmers mechanism provides closer agreement with measurements at 55atm compared to the other two mechanisms. More importantly, the Chalmers mechanism is able to capture the negative temperature coefficient (NTC) regime at 55atm, where the ignition delay time increases with temperature. The NTC regime is indicated more clearly in Fig. 2, which compares the Chalmers predictions with measurements for various pressure ranges and covering ignition delay times over two orders of magnitude. Again, the Chalmers mechanism is able to capture the experimentally observed effects of pressure and temperature on the ignition delay, including NTC regime [45]. Based on this comparison, the Chalmers mechanism was employed to characterize the effect of H_2 addition on the ignition of n-C_7H_{16}–air mixtures.

A similar validation study was performed for the Chalmers mechanism to predict the ignition delays for CH_4–air mixtures at engine relevant conditions. Figure 3 compares the predicted ignition delays, using the GRI 3.0 [46] and Chalmers mechanisms, with the experimental data of Ref. [23, 47]. Again, while both the mechanisms exhibit discrepancies, the Chalmers mechanism provides reasonable agreement with measurements, especially at

moderate to low temperatures. Additional validation results for CH_4/air and CH_4–H_2/air mixtures have been reported in Refs. [23, 48, 49].

3. Results and Discussion

Having validated the Chalmers mechanism against the ignition data at high pressures, results now focus on characterizing the effect of ignition behavior of n-C_7H_{16}/H_2 and n-C_7H_{16}/CH_4 blends. Here, the effects of H_2 or CH_4 addition on the ignition of n-C_7H_{16}–air mixture, as well as that of n-C_7H_{16} addition on the ignition of H_2–air or CH_4–air mixtures are presented. In addition, results of a sensitivity study performed to identify the dominant reactions associated with the ignition of these blends at engine relevant conditions are discussed.

3.1 Ignition of n-C_7H_{16}/H_2–air Mixtures

Figure 4 presents the effect of H_2 addition on the ignition of n-C_7H_{16}–air mixtures under different pressure and stoichiometric conditions. Results are shown in terms of the plot of ignition delay time as a function of temperature for pressures of 55 and 33 atm, ϕ=1 and 2, and three different n-C_7H_{16}–H_2 blends with 0%, 20%, and 80% H_2 by volume. For all these cases, the effect of H_2 appears to be small, especially at temperatures above 1000K. For temperatures below 1000K, the ignition delay for all three blends exhibits the NTC behavior. In addition, as the amount of H_2 in the blend is increased, t_{ign} first decreases (for 20% H_2) and then increases (for 80% H_2). This seems to imply that for 80% or higher H_2 in the blend, the ignition behavior is increasingly influenced by the H_2 oxidation chemistry. In order to examine this aspect further, the ignition delay times for blends with H_2 content varying from 0 to 100% are plotted in Fig. 5. As the amount of H_2 in the blend exceeds 80%, the ignition delay time decreases for temperatures above 1000K, but increases for lower temperatures. Moreover, the ignition delay exhibits a smooth transition to that of 100% H_2 as the mole fraction of H_2 in the blend is continuously increased. The ability of the Chalmers mechanism to predict the ignition behavior of H_2–air mixtures and n-C_7H_{16}–H_2 blends was further assessed by comparing its predictions with those using the Dryer [37] and Connaire [50] mechanisms for H_2–air mixtures, and with the LLNL mechanism [44] for different n-C_7H_{16}–H_2 blends. Note that the Connaire mechanism has been extensively validated for H_2 oxidation using a variety of targets. Results for the ignition of H_2–air mixture at ϕ=1, p=55 atm are presented in Fig. 6, and clearly demonstrate the

ability of Chalmers mechanism to capture the H_2 ignition chemistry under engine relevant conditions. Similarly, the comparison of ignition delay times predicted using the Chalmers and LLNL mechanism for three different n-C_7H_{16}–H_2 blends provides further validation for predicting the ignition behavior of n-C_7H_{16}–H_2 blends under engine relevant conditions.

To summarize the results so far, for H_2 content below 80%, the addition of H_2 has a negligible effect on the ignition of n-heptane-air mixtures, while for H_2 above 80%, the ignition behavior is increasingly influenced by the H_2 oxidation chemistry. For the latter case, the H_2 addition increases and decreases the ignition delay time for temperatures above and below 1000K, respectively. Another way to interpret these results is that a relatively small amount of n-C_7H_{16} can significantly modify the ignition behavior of H_2-air mixtures. The n-C_7H_{16} addition increases and decreases the ignition delay time for H_2-air mixtures for temperatures above and below 1000K, respectively.

3.2 Results of Sensitivity Study

A sensitivity study was performed to identify the dominant reactions associated with the ignition of n-C_7H_{16}/H_2 blends at conditions relevant to diesel and HCCI engines in terms of pressure, temperature, and equivalence ratio. Important reactions identified from the sensitivity analysis along with their kinetic parameters are listed in Table I. Figure 8 presents normalized sensitivity coefficients with respect to various reactions for the ignition of three different n-C_7H_{16}-H_2 blends at ϕ=2, T=800K, and p=30 and 55 atm. For these conditions, the effect of H_2 appears to be small, consistent with the results discussed above. For the 0%H_2 case, R12, R90, and R25 appear to be the important reactions. Reaction R12 ($C_7H_{14}O_2H+O_2=C_7H_{14}O_2HO_2$) is an important branching reaction, which transforms the alkyl-hydroperoxy radical into the peroxy-alkylhydroperoxy radical. This path promotes the formation of ketohydroperoxide species that are the branching agents producing new radicals, such as $C_5H_{11}CHO$ and CH_2O. Reaction R90 ($H_2O_2+m=OH+OH+m$) involves the formation of two OH radicals, which clearly enhances system reactivity and reduces ignition delay. On the contrary the decomposition reaction R25 (C_7H_{15}-2 = C_4H_9+ C_3H_6) reduces the possibility to form the corresponding alkyl-peroxy radical (C_7H_{15}-OO), thus decreasing system reactivity and increasing ignition delay. Furthermore, as indicated in Figure 8, the sensitivity to these three reactions increases as the amount of H_2 in the blend is increased, while it decreases as the

pressure is increased from 30 to 55 atm. In addition, reaction R71 (H_2+OH=H_2O+H) decreases the system reactivity and seems to become important at higher pressure as the amount of H_2 in the blend is increased.

Figure 9 depicts the effect of temperature on the normalized sensitivity coefficients for the 80%H_2/20%C_7H_{16} case at p=55 atm, and ϕ=2 and 0.5. As the temperature is reduced from 1000 to 800K, the sensitivity to reactions R6, R12, R90, and R25 decreases for the fuel rich condition. Note that R6 involves the formation of the heptyl radical (C_7H_{15}-2), which enhances system reactivity. For the lean condition (ϕ=0.5), the sensitivity to reactions R6, R12, and R25 decreases, while that to R90 increases as the temperature is decreased. In addition, reaction R103 (CH_2O+OH=HCO+H_2O) becomes important for lean mixtures at T=800K. The NTC behavior discussed in the context of Fig. 1 may partially be attributed to the increased sensitivity to reactions R71 and R103, both of which consume the hydroxyl radical, and become important at 800K and ϕ=0.5. Other observation from Figs. 8 and 9 is that the effect of pressure on the sensitivity coefficients is relatively small compared to those of temperature and equivalence ratio. While R6, R12, R90, and R25 appear to be the important reactions in general, reactions R71, R90 and R103 also play a more significant role for leaner mixtures (ϕ=0.5) and at lower temperatures (T=800K).

As discussed earlier, an important result in the context of Fig. 5 pertains to the significant effect caused by the addition of a relatively small amount of n-C_7H_{16} on the ignition of H_2–air mixtures. This aspect is further examined here through a sensitivity analysis. Figure 10 presents the normalized sensitivity coefficients for the ignition of two mixtures, one with 100%H_2 and the other with 5%C_7H_{16}/95%H_2 blend, at ϕ=1, T=900K, and p=30 and 55 atm. For the 100%H_2 case, the important reactions are R90, R91, R70, R96, and R89. These reactions, which involve species such as H_2O_2, HO_2, H_2, OH, etc., are known to be associated with H_2 ignition, and have been extensively discussed, particularly in the context of H_2 explosion and ignition limits, by several researchers; see, for example, Law and coworkers [51, 52], Briones et al. [53], and Aggarwal and Briones [54]. For the case with 5% n-C_7H_{16} in the blend, the relative importance of these reactions decreases appreciably, while reactions R12, R4, R71, R25, and R6 become important. These reactions, except for R71, are associated with the pyrolysis/oxidation of n-C_7H_{16}. Thus the noticeable reduction in the ignition delay of H_2–

air mixtures caused by the addition of n-C_7H_{16} at low temperatures can be attributed to the emergence of reactions R12, R4, and R6. Both reactions R4 and R6 involve the formation of heptyl radical (C_7H_{15}-2), which subsequently form heptyl-peroxy radical and then heptyl-hydroperoxy radical, with the latter species involved in reaction R12 as discussed earlier.

It is also interesting to note that our results are generally in accord with those reported by Subramanian et al. [40] concerning the effect of H_2 addition on the ignition of n-C_7H_{16}–air mixtures. Specifically in both the studies, the addition of H_2 is observed to lengthen the ignition delay at low temperatures, and can mainly be attributed to reaction R71 (H_2+OH = H_2O+H) that transforms OH radicals into H radicals, and subsequently produces HO_2 by reaction H + O_2 = HO_2. However, our results further indicate that this effect is observed when the H_2 mole fraction in the n-C_7H_{16}/H_2 blend is more that 80%. On the other hand, the addition of a relatively small amount of n-heptane to H_2–air mixtures considerably shortens the ignition delay, and can be attributed to the production of heptyl radical through reactions R4 and R6, which subsequently leads to the formation of heptyl-hydroperoxy radical as mentioned earlier.

3.3 Ignition of n-C_7H_{16}/CH_4–air Mixtures

Figure 11 presents the effect of CH_4 addition on the ignition of n-C_7H_{16}–air mixtures under different pressure and stoichiometric conditions. Results are shown in terms of the plot of ignition delay time as a function of temperature for pressures of 33 and 55 atm, ϕ=1 and 0.5, and five different n-C_7H_{16}–CH_4 blends with 0%, 20%, 80%, 95%, and 100% CH_4 by volume. For the 20% and 80% CH_4 cases, the effect of CH_4 on the ignition of n-C_7H_{16} appears to be small, implying that the ignition behavior is dominated by the ignition chemistry of n-C_7H_{16}. Thus, similar to the results for n-C_7H_{16}–H_2 blends, the ignition delay exhibits the NTC behavior, i.e., the ignition delay time increases as the temperature is increased. The effect of CH_4 addition seems to become more noticeable as the amount of CH_4 in the blend exceeds 80%. Another way to interpret these results is in terms of the effect of n-heptane on the ignition of CH_4-air mixtures. As indicated in Fig. 11, the addition of n-C_7H_{16} decreases the ignition delay for CH_4-air mixtures for both low and high temperature conditions. It is interesting to compare this result to that for H_2-air mixtures for which the addition of n-C_7H_{16} increases the ignition delay at high temperatures, but decreases it at low temperatures.

It is also important to note that the ignition or pyrolysis/oxidation chemistry of methane is known to be slow compared to that of higher hydrocarbon fuels including *n*-heptane, an evidence of which is by the minimum ignition temperature and ignition delay data reported in [55, 56, 57, 58]. As discussed in Refs. [55, 56], the autoignition temperatures of methane/air and *n*-heptane/air mixtures at 1 atm are 810 and 477 K, respectively. In addition, the shock tube data reported by Horning et al. [57] and Hidaka et al. [58] indicate that the ignition delay times for methane/air and n-heptane/air mixtures under similar conditions are 0.8 and 0.16 ms, respectively. Our results presented above are in accord with this data.

4. Conclusions

A numerical investigation has been conducted to examine the effects of hydrogen and methane on the ignition of n-heptane-air mixtures. The CHEMKIN 4.1 suite of software has been used to perform simulations for a closed homogenous reactor under conditions relevant to diesel and HCCI engines. The parameters include temperature in the range of 800-1400K, pressures of 30 and 55 atm, and equivalence ratio in the range of 0.5-2.0. Shock tube ignition data has been used to validate the ignition delay times for n-C_7H_{16}/air mixtures predicted using three reaction mechanisms, namely (i) NIST mechanism involving 203 species and 1463 reactions, (ii) Dryer mechanism consisting of 116 species and 754 reactions, and (iii) Chalmers mechanism with 42 species and 168 reactions. Some results for the ignition of n-C_7H_{16}/H_2 blends using the LLNL mechanism (version 3) are also presented. The Chalmers mechanism was found to provide closer agreement with measurements compared to the other two mechanisms, particularly at high pressures (p=55atm). Moreover, it was able to reproduce the experimentally observed negative temperature coefficient (NTC) regime, which was not captured by the other two mechanisms. The Chalmers mechanism was further validated for predicting the ignition characteristics of H_2/air and CH_4/air mixtures at engine relevant conditions. Based on these validations, this mechanism was employed to characterize the ignition behavior of n-C_7H_{16}/H_2 and n-C_7H_{16}/CH_4 fuel blends. Important observations are as follows.

For the conditions investigated, the addition H_2 or CH_4 has a relatively small effect on the ignition of n-C_7H_{16}/air mixtures. Even with 80% H_2 or CH_4 (by volume) in the blend, the ignition behavior is strongly influenced by the n-C_7H_{16} oxidation chemistry. On the other hand,

the addition of a relatively small amount of n-C_7H_{16} to H_2/air and CH_4/air mixtures is found to significantly modify their ignition characteristics. While the addition of n-C_7H_{16} to H_2/air mixtures decreases and increases the ignition delays at low and high temperatures, respectively, its addition to CH_4/air mixtures decreases ignition delays at all temperatures. These results may be interesting from the perspective of using n-heptane (or diesel fuel) in modifying the ignition and combustion characteristics of hydrogen-fueled and natural gas-fueled engines. For instance, in a dual-fuel, dual-injection engine, the diesel fuel may be injected prior to introducing the liquefied natural gas.

A sensitivity analysis was performed to identify the important reactions associated with the ignition of n-C_7H_{16}/H_2 blends at engine relevant conditions. Important reactions identified include R12 ($C_7H_{14}O_2H+O_2=C_7H_{14}O_2HO_2$), R90 ($H_2O_2+m=OH+OH+m$), and R25 ($C_7H_{15}$-2= $C_4H_9+ C_3H_6$). The sensitivity to these reactions increases as the amount of H_2 in the blend is increased. In addition, reactions R71 ($H_2+OH=H_2O+H$), R6 ($C_7H_{16}+HO_2=C_7H_{15}$-2+H_2O_2), and R103 ($CH_2O+OH=HCO+H_2O$) becomes important at certain conditions. Overall, the heptyl and hydroxyl radicals play a key role in determining the ignition behavior of n-C_7H_{16}/H_2 and n-C_7H_{16}/CH_4 blends.

Acknowledgments

Authors greatly appreciate many insights provided by Dr. Eliseo Ranzi of Politecnico di Milano. This work was partially supported by the U.S. Department of Energy Office of Vehicle Technology under the management of Mr. Gurpreet Singh. The paper is devoted to the memory of Mr. O. Awomolo whose life was suddenly taken away by some senseless violence in Chicago.

References

1. Aggarwal SK, Hydrogen-Assisted Combustion and Emission Characteristics of Fossil Fuels, Book Chapter, Handbook of Combustion, Volume 3, Edited by, M. Lackner, F. Winter, and A. K. Agarwal, Verlag GmbH, Weinheim, ISBN 978-3-527-32449-1, 2010.
2. Cho HM, He B-Q. Spark ignition natural gas engines—A review, Energy Conversion & Management 2007;48 (2):608-18.
3. Hountalas DT, Papagiannakis RG. A simulation model for the combustion process of natural gas engines with pilot diesel fuel as an ignition source. 2001: SAE Paper: 2001-01-1245.

4. Agarwal A, Assanis D. Multi-dimensional modeling of ignition, combustion and nitric oxide formation in direct injection natural gas engines. 2000; SAE paper; 2000-01-1839.
5. Beck NJ, Barkhimer RL, Johnson WP, Wong HC, Gebert K. Evolution of heavy duty natural gas engines - stoichiometric, carbureted and spark ignited to lean burn, fuel injected and micro-pilot. 1997;SAE paper 972665.
6. Guo H, Smallwood GJ, Liu F, Ju Y, Gulder OL. The effect of hydrogen addition on flammability limit and NOx emission in ultra-lean counterflow CH4/air premixed flames. Proc. Combust Inst 2005; 30:303-11.
7. Yu G, Law CK, Wu CK. Laminar flame speeds of hydrocarbon + air mixtures with hydrogen addition. Combust Flame 1986;63:339-47.
8. Halter F, Chauveau C, Djebaıli-Chaumeix N, Gokalp I. Characterization of the effects of pressure and hydrogen concentration on laminar burning velocities of methane–hydrogen–air mixtures. Proc. Combust Inst 2005;30:201-8.
9. Shy SS, Chen YC, Yang CH, Liu CC, Huang CM. Effects of H2 or CO2 addition, equivalence ratio, and turbulent straining on turbulent burning velocities for lean premixed methane combustion Combust Flame 2008;153:510-24.
10. Briones AM, Aggarwal SK, Katta VR. Effects of H2 Enrichment on The Propagation Characteristics of CH4-Air Triple Flames. Combust Flame 2008;153:367-83.
11. Tuncer O, Acharya S, Uhm JH. Dynamics, NOx and flashback characteristics of confined premixed hydrogen-enriched methane flames. Int. J Hydrogen Energy 2009; 34:496-506.
12. Naha S, Aggarwal SK. Fuel effects on NOx emissions in partially premixed flames. Combust Flame 2004; 39: 90-105.
13. Naha S, Briones AM, Aggarwal SK. Effect of fuel blends on pollutants emissions in flames. Combust Sci Technol 2005;177(1):183-220.
14. Guo H, Neill WS. A numerical study on the effect of hydrogen/reformate gas addition on flame temperature and NO formation in strained methane/air diffusion flames Combust Flame 2009;156: 477-83.
15. Schefer RW, Wicksall DM, Agrawal AK. Combustion of hydrogen-enriched methane in a lean premixed swirl-stabilized burner. Proc. Combust Inst 2002;29:843-51.
16. Schefer RW. Hydrogen enrichment for improved lean flame stability. Int J Hydrogen Energy 2003;28:1131-41.
17. Halter F, Chauveau C. Gokalp I. Characterization of the effects of hydrogen addition in premixed methane/air flames. Int. J Hydrogen Energy 2007;32:2585-92.

18. Choudhuri AR, Gollahalli SR. Characteristics of hydrogen–hydrocarbon composite fuel turbulent jet flames. Int J Hydrogen Energy 2003;28:445-454.
19. Kim HS, Arghode VK, Linck MB, Gupta AK. Hydrogen addition effects in a confined swirl-stabilized methane-air flame. Int J Hydrogen Energy 2009;34:1045-53.
20. Kahraman N, Ceper B, Akansu SO, Aydin K. Investigation of combustion characteristics and emissions in a spark-ignition engine fuelled with natural gas–hydrogen blends. Int J Hydrogen Energy 2009;34(2):1026-34.
21. Shirk MG, McGuire TP, Neal GL, Haworth DC. Investigation of a hydrogen-assisted combustion system for a light-duty diesel vehicle. Int J Hydrogen Energy 2008;33:7237-44.
22. Gersen S, Anikin NB, Mokhova AV, Levinsky HB. Ignition properties of methane/hydrogen mixtures in a rapid compression machine. Int J Hydrogen Energy 2008;33:1957-64.
23. Huang J, Bushe WK, Hill P G, Munshi SR. Shock initiated ignition in homogeneous methane-hydrogen-air mixtures at high pressure. Int. J. of Chemical Kinetics 2006;38(4):221-33.
24. Fotache CG, Kreutz TG, Law CK. Ignition of hydrogen-enriched methane by heated air. Combust Flame 1997;110:429-40.
25. Safta C, Madnia CK. Autoignition and structure of nonpremixed CH4/H2 flames: Detailed and reduced kinetic models. Combust Flame 2006;144:64-73.
26. Ju Y, Niioka T. Reduced kinetic mechanism of ignition for nonpremixed hydrogen/air in a supersonic mixing layer. Combust Flame 1994;99:240-6.
27. Herzler J, Jerig L, Roth P. Shock tube study of the ignition of lean n-heptane/air mixtures at intermediate temperatures and high pressures. Proc. Combust Inst 2005;30:1147-53.
28. Gauthier BM, Davidson DF, Hanson RK. Shock tube determination of ignition delay times in full-blend and surrogate fuel mixtures. Combust Flame 2004;139(4):300-11.
29. Xue H, Aggarwal SK. The structure and extinction of heptane/Air partially-premixed flames. AIAA Journal 2002;40(11):2289-97.
30. Xue H, Aggarwal SK. NOx emissions in n-heptane/air partially premixed flames. Combust Flame 2003;132:723-41.
31. Berta P, Puri IK, Aggarwal SK. An experimental and numerical investigation of n-heptane/air counterflow partially premixed flames and emission of NOx and PAH species. Combust Flame 2006;145:740-64.

32. Katta VR, Aggarwal SK, and Roquemore WM. Evaluation of Chemical-Kinetics Models for n-Heptane Combustion Using a Multidimensional CFD Code, Fuel, Submitted, 2011.
33. Tsang W. Data Science Journal, 3:1-9 (2004).
34. http://www-mae.ucsd.edu/~combustion/cermech/Heptane-Reactions/
35. http://www-cmls.llnl.gov/?url=science_and_technology-chemistry-combustion-c7h16_reduced_mechanism.
36. Curran HJ, Gaffuri P, Pitz WJ, Westbrook CK. A comprehensive modeling study of n-heptane oxidation. Combust Flame 1998;114:149-77.
37. Chaos M, Kazakov A, Zhao Z, Dryer FL. A high-temperature chemical kinetic model for primary reference fuels. Int J of Chemical Kinetics 2007;39(7):399-414.
38. Goldaniga A, Faravelli T, Ranzi E. The kinetic modeling of soot precursors in a butadiene flame. Combust Flame 2008;122(3):350-8.
39. http://www.tfd.chalmers.se/~valeri/MECH.html
40. Subramanian G, Da Cruz AP, Bounaceur R, Vervisch L. Chemical impact of CO and H2 addition on the auto-ignition delay of homogeneous n-heptane/air mixtures. Combust. Sci. Technol. 2007;179:1937-62.
41. Thiessen S, Khalil E, Karim G. The autoignition in air of some binary fuel mixtures containing hydrogen. Int J Hydrogen Energy 2010;35:10013-7.
42. Saravanan N, Nagarajan G. Experimental investigation in optimizing the hydrogen fuel on a hydrogen diesel dual-fuel engine. Energy Fuel 2009;23:2646-57.
43. Kee RJ, Rupley FM, Miller JA. CHEMKIN Collection, Release 3.6 ed., Reaction Design Inc., San Diego, CA, 2000.
44. Mehl M, Curran HJ, Pitz WJ, Westbrook CK. Chemical kinetic modeling of component mixtures relevant to gasoline, European Combustion Meeting, Vienna, Austria, 2009.
45. Cieszki HK, Adomeit G. Shock tube investigation on self-ignition of n-heptane air mixtures under engine relevant conditions, Combust Flame 1993;93:421-33.
46. Smith GP, Golden DM, Frenklach M, Moriarty NW, Eiteneer B, Goldenberg M, Bowman CT, Hanson RK, Song S, Gardiner Jr. WC, Lissianski VV, Qin Z. GRI Mech-3.0: http://www.me.berkeley.edu/grimech/
47. Seery DJ, Bowman CT. An experimental and analytical study of methane oxidation behind shock waves. Combust Flame 1970;14:37-47.

48. Som S, Sivaramakrishnan R, Brezinsky K, Aggarwal SK. Validation of a Detailed Chemical Kinetic Model for the High Pressure Combustion of Methane-Flame and Ignition Characteristics, Fifth U.S. National Combustion Meeting, San Diego, CA, March 2007.
49. Adhikary BD, Aggarwal SK, and Katta VR. Ignition of Methane-Hydrogen and Heptane-Hydrogen Mixtures at High Pressures, Sixth U.S. National Combustion Meeting, Ann Arbor, Michigan, May 17-20, 2009.
50. O'Connaire M, Curran HJ, Simmie JM, Pitz WJ, Westbrook CK. A Comprehensive modeling study of hydrogen oxidation. Int J Chem Kinetics 2004;36:603-22.
51. Fotache CG, Kreutz TG, Law CK. Ignition of hydrogen-enriched methane by heated air. Combust Flame 1997;110:429-40.
52. Zheng XL, Law CK. Ignition of premixed hydrogen/air by heated counterflow under reduced and elevated pressures. Combust Flame 2004;136:168-79.
53. Briones AM, Puri IK, Aggarwal SK. Effect of pressure on counterflow H2-air partially premixed flames. Combust Flame 2005;140:46-59.
54. Aggarwal, SK, Briones A. Hydrogen combustion and emissions in a sustainable energy future, Handbook of Combustion, Edited by, M. Lackner, F. Winter, and A. K. Agarwal, Wiley-VCH Verlag GmbH, Weinheim, ISBN 978-3-527-32449-1, April 2010.
55. Material Safety Data Sheet (MSDS) for methane (CH4), Voltaix, Inc., Post Office Box 5357, North Branch, NJ 08876-5357, USA, 1994 (Revised 1996).
56. Material Safety Data Sheet (MSDS) for heptane, Matheson Tri-Gas, Inc., 959 Route 46 East Chemtrec 1-800-424-9300, Parsippany, NJ 07054-0624, USA, 1989 (Revised 2002).
57. Horning DC, Davidson DF, Hanson RK. Study of the high-temperature autoignition of n-alkane/O/Ar mixtures. J Propulsion Power 2002;18 (2):363-71.
58. Hidaka Y, Sato K, Henmi Y, Tanaka H, Inami K. Shock-tube and modeling study of methane pyrolysis and oxidation. Combust Flame 1999;118:340-58.

List of Tables

List of Figures

Figure 9: Normalized sensitivity coefficients for the ignition of n-heptane/hydrogen blend (20%/80% by volume) at 55 atm, ϕ=2 (Fig. a) and ϕ=0.5 (Fig. b), and temperature of 800K (Blue) & 1000K (Red).

Figure 10: Normalized sensitivity coefficients for the ignition of (a) H_2–air mixture, and (b) 5%n-C_7H_{16}/95%H_2–air mixture at a temperature of 900K, ϕ=1, and pressures of 30 atm (Blue) and 55 atm (Red).

Figure 11: Predicted ignition delay time plotted versus the inverse of temperature for five different n-C_7H_{16}–CH_4 blends with 0% CH_4 (Circle), 20% CH_4 (Square), 80% CH_4 (Triangle), 95% CH_4 (Diamond) & 100% CH_4 (Cross Symbol). Other conditions are p=30 atm and ϕ=1 (Fig. a), p=55 atm and ϕ=1 (Fig. b), and p=55 atm and ϕ=0.5, (Fig. c).

Table I: Important reactions determined from sensitivity analysis.

#	Reactions	A	b	E
4	c7h16+oh=c7h15-2+h2o	4.50E+9	1.3	690.5
5	c7h16+ho2=c7h15-1+h2o2	1.12E+13	0	19300
6	c7h16+ho2=c7h15-2+h2o2	1.65E+13	0	16950
8	c7h16+o2=c7h15-2+ho2	2.00E+14	0	47380
12	c7h14o2h+o2=c7h14o2ho2	4.60E+11	0	0
24	c7h15-1=c2h4+c5h11	2.50E+13	0	28810
25	c7h15-2=c4h9+c3h6	2.20E+13	0	28100
44	ch3o+o2=ch2o+ho2	1.20E+11	0	2600
45	ch3+ho2=ch3o+oh	5.00E+13	0	0
47	ch3+o2=ch2o+oh	3.80E+11	0	9000
70	h2 + o2=oh+oh	1.70E+13	0	47780
71	h2+oh=h2o+h	1.17E+09	1.3	3626
72	o+oh=o2+h	8.00E+14	-0.5	0
76	h+o2+m=ho2+m	3.60E+17	-0.7	0
89	ho2+ho2=h2o2+o2	2.00E+12	0	0
90	h2o2+m=oh+oh+m	4.30E+16	0	45500
91	h2o2+h=ho2+h2	6.5E+11	0	3800
96	h2 + ho2=h2o+oh	1.6E+12	0	18800
103	ch2o+oh=hco+h2o	2.43E+10	1.2	-447
104	ch2o+ho2=hco+h2o2	3.00E+12	0	8000
125	ch3+ch3o=ch4+ch2o	4.30E+14	0	0
146	c2h4+oh=ch2o+ch3	6.00E+13	0	960

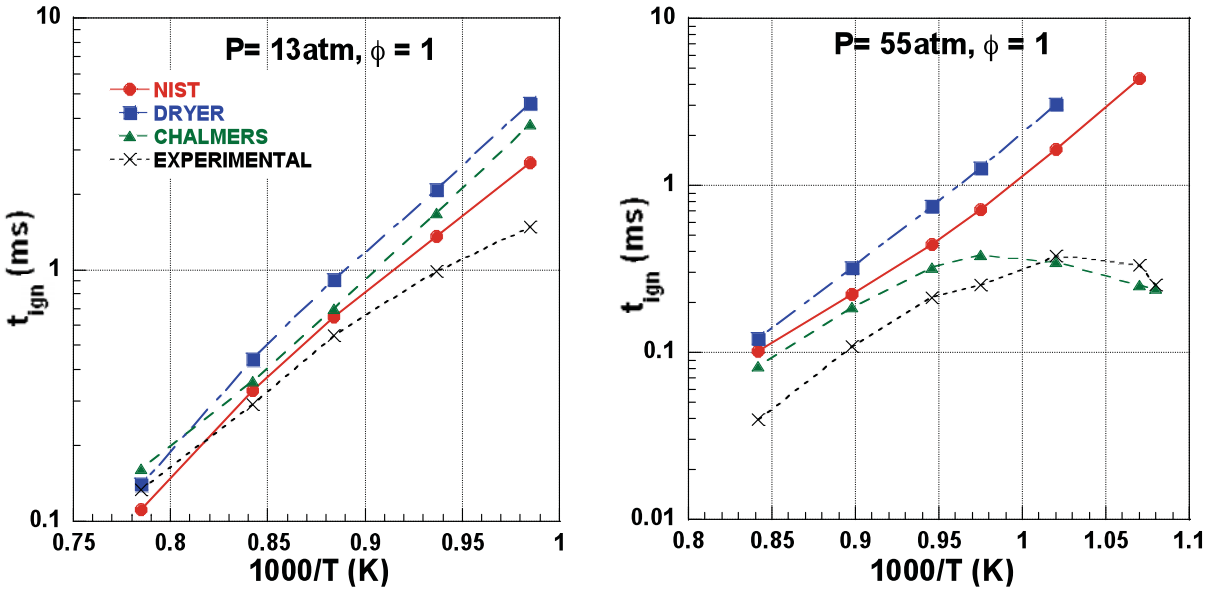

Figure 1: Measured and predicted ignition delay times for n-C_7H_{16}–air mixtures at pressures of 13 atm (Fig a) and 55 atm (Fig b) and equivalence ratio ϕ=1. Measurements (cross) are from Gauthier et al. [28] and predictions are based on the NIST (circle), Dryer (square), and Chalmers (triangle) mechanisms.

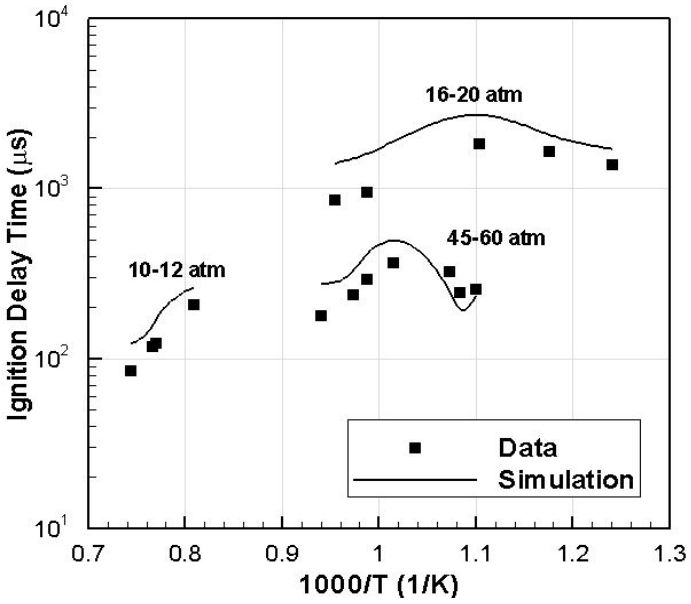

Figure 2: Comparison of predictions using the Chalmers mechanism with the measurements of Gauthier et al. [28] for ignition delay times as a function of temperature for stoichiometric (ϕ=1) n-heptane/air mixtures at different pressures.

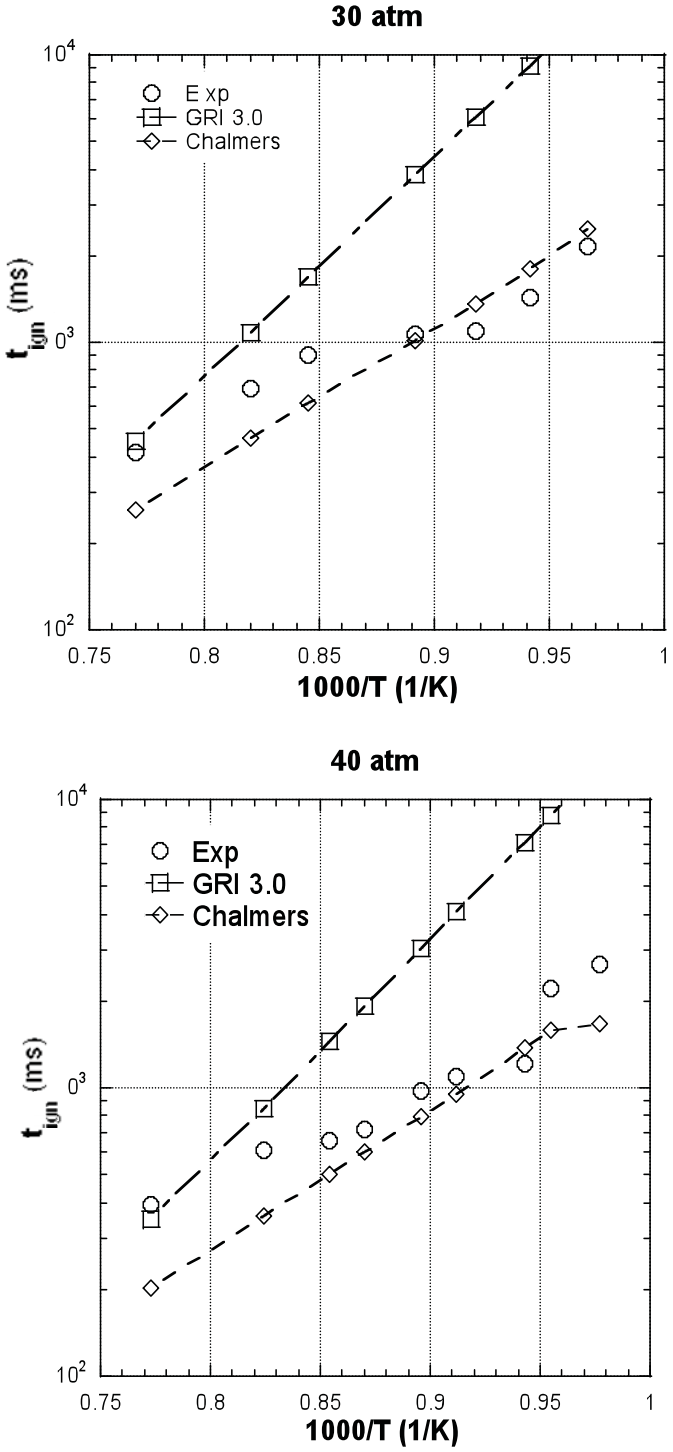

Figure 3: Comparison of predictions using the GRI 3.0 and Chalmers mechanisms with the measurements of Ref. [23] for ignition delay times as a function of temperature for stoichiometric (ϕ=1) methane/air mixtures at two different pressures.

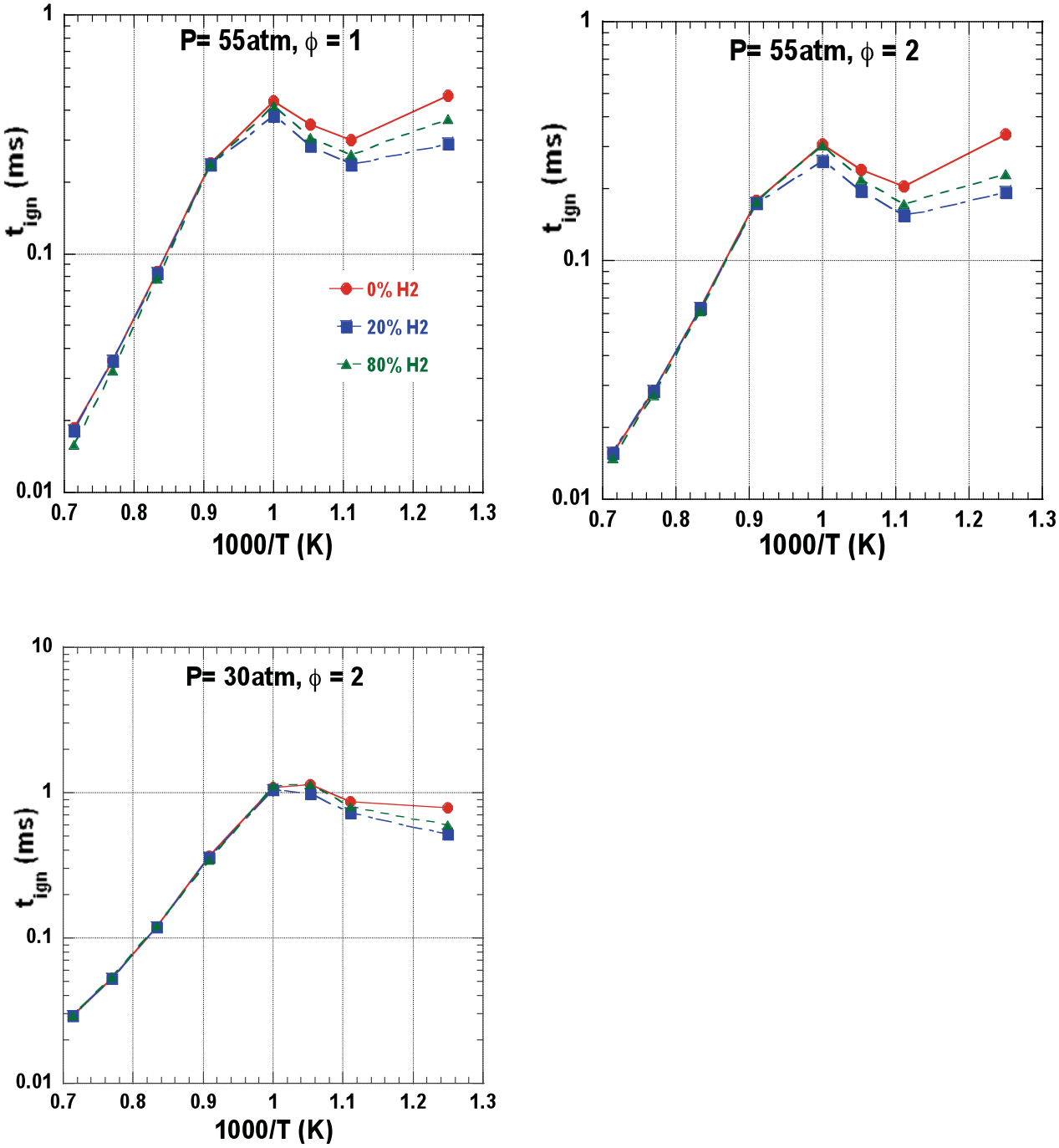

Figure 4: Predicted ignition delay time plotted versus the inverse of temperature for three different n-C_7H_{16}–H_2 blends with 0% H_2 (Circle), 20% H_2 (Square), and 80% H_2 (Triangle). Other conditions are p=55 atm and ϕ=1 (Fig. a), p=55 atm and ϕ=2 (Fig. b), p=30 atm and ϕ=2, (Fig. c).

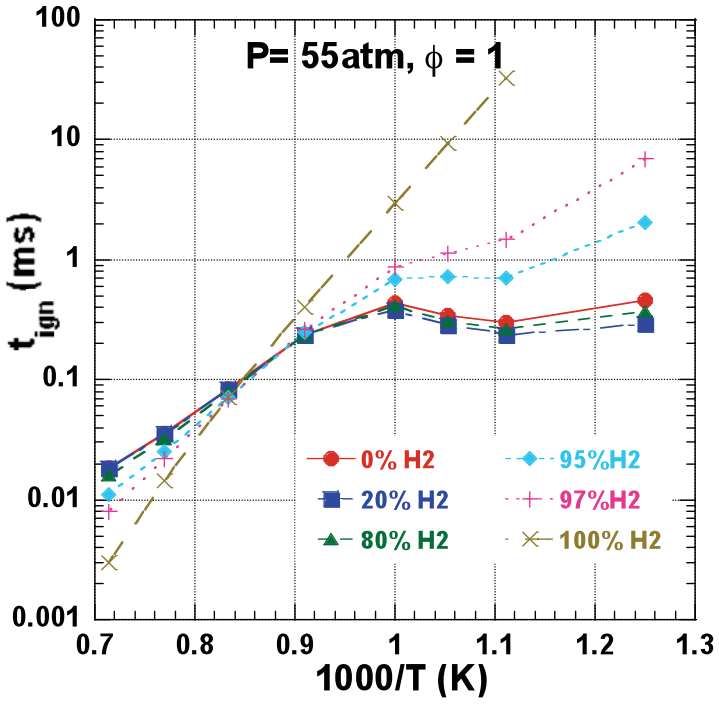

Figure 5: Predicted ignition delay time versus the inverse of temperature for ϕ=1, p=55 atm, and different n-C_7H_{16}–H_2 blends with 0% H_2 (Circle), 20% H_2 (Square), 80% H_2 (Triangle), 95% H_2 (Diamond), 97% H_2 (Plus symbol), and 100% H_2 (Cross) by volume.

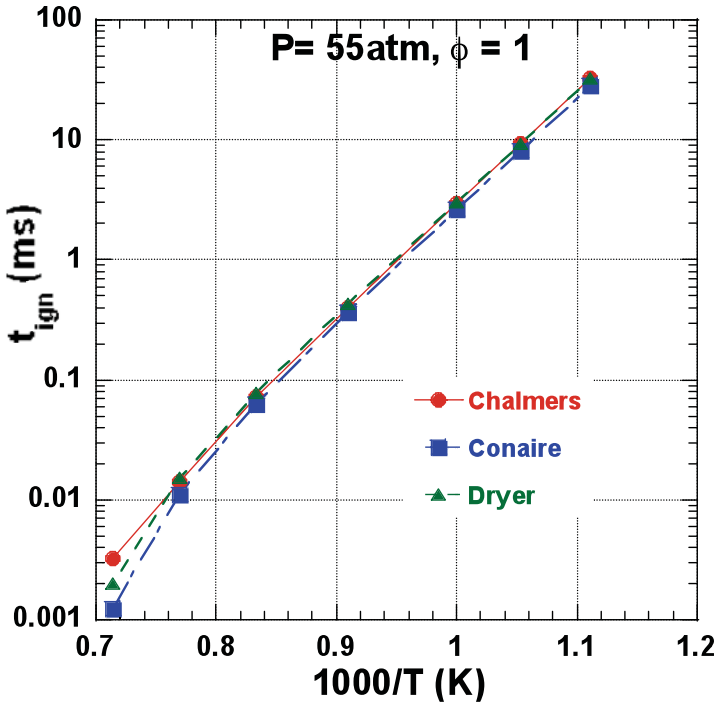

Figure 6: Predicted ignition delay times plotted versus the inverse of temperature for H_2–air mixture at ϕ=1, p=55 atm. Predictions are based on the Chalmers, Conaire, and Dryer mechanisms.

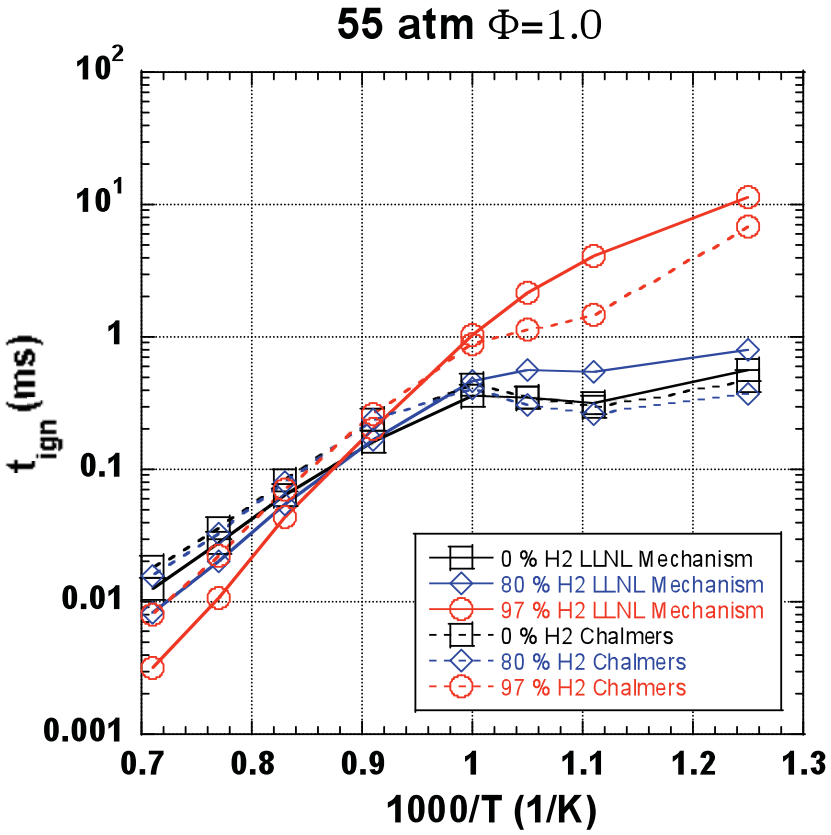

Figure 7: Comparison of ignition delay times computed using the Chalmers and LLNL (Version 3) mechanisms for three different n-C_7H_{16}–H_2 blends (with 0% H_2, 80% H_2, 97% H_2 by volume) at ϕ=1, p=55 atm.

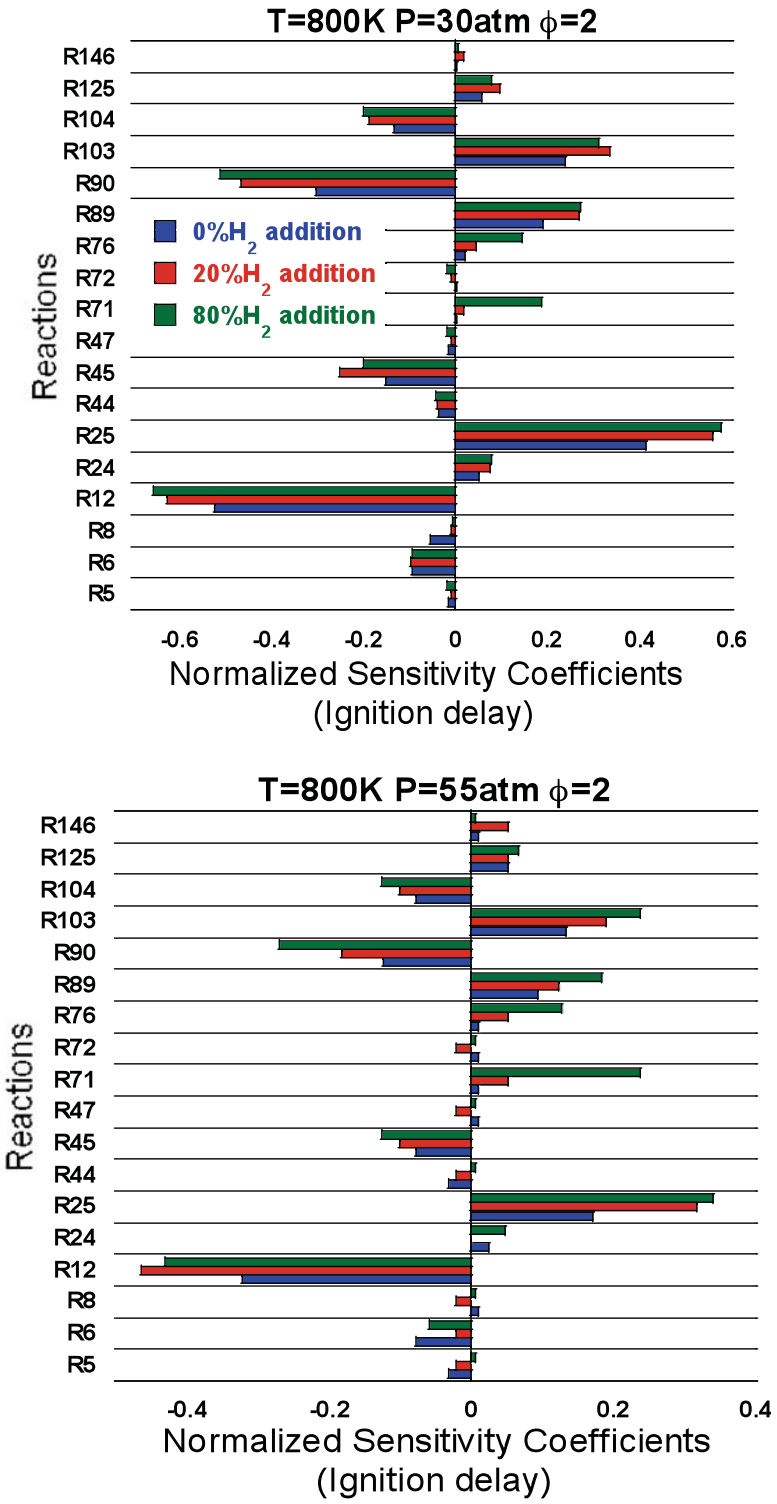

Figure 8: Normalized sensitivity coefficients for the ignition of three different n-heptane/hydrogen blends at ϕ=2, temperature=800K, and pressures of 30 atm and 55 atm. Three blends are with 0% (blue), 20% (red), and 80% by volume (green).

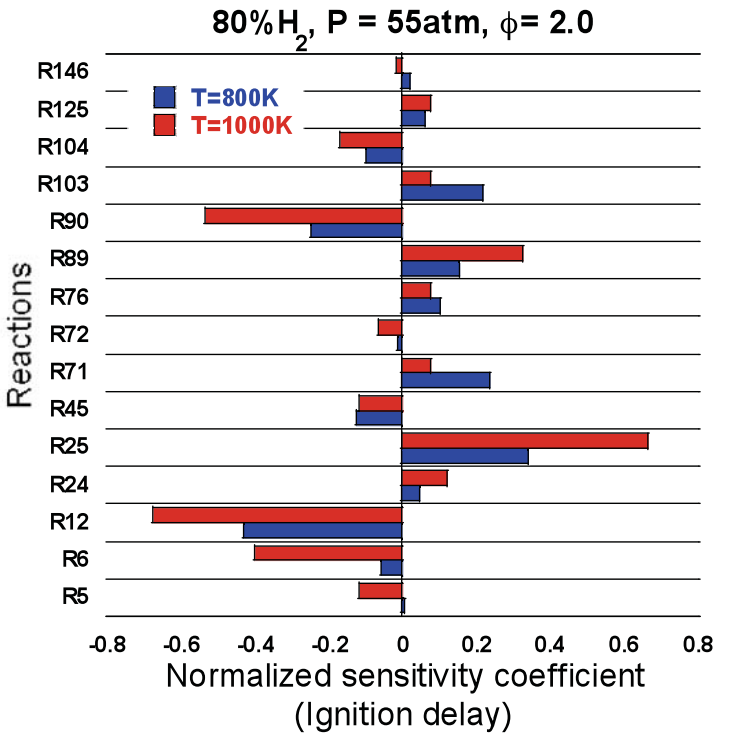

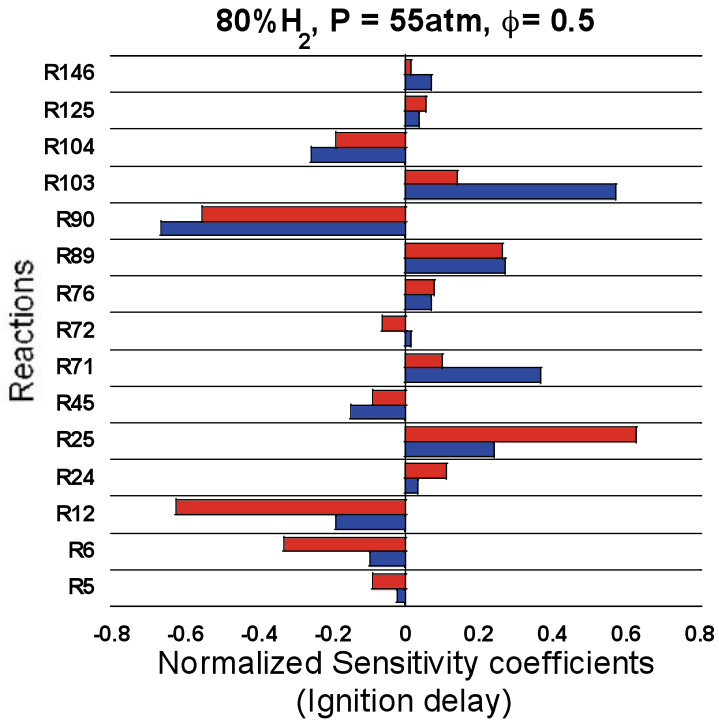

Figure 9: Normalized sensitivity coefficients for the ignition of n-heptane/hydrogen blend (20%/80% by volume) at 55 atm, ϕ=2 (Fig. a) and ϕ=0.5 (Fig. b), and temperature of 800K (Blue) & 1000K (Red).

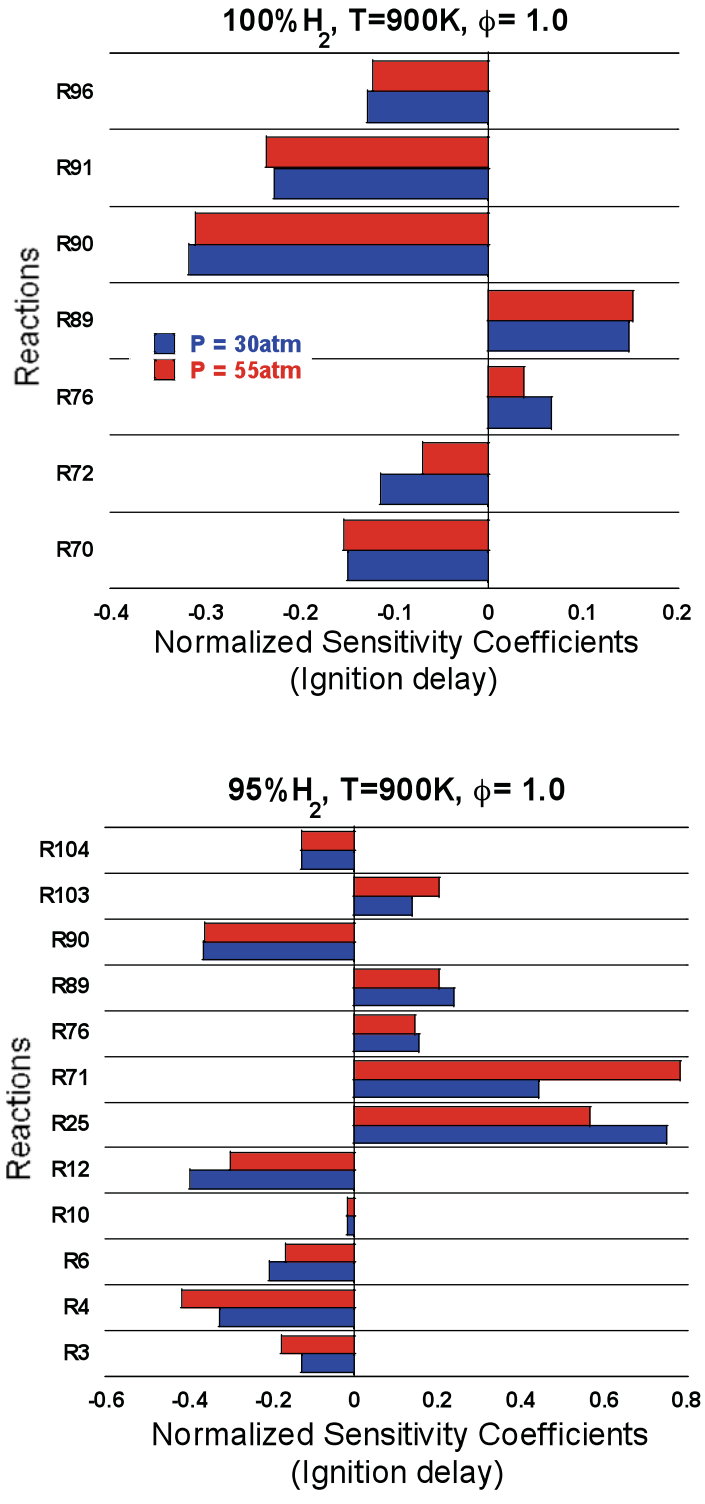

Figure 10: Normalized sensitivity coefficients for the ignition of (a) H_2–air mixture, and (b) 5%n-C_7H_{16}/95%H_2–air mixture at a temperature of 900K, ϕ=1, and pressures of 30 atm (Blue) and 55 atm (Red).

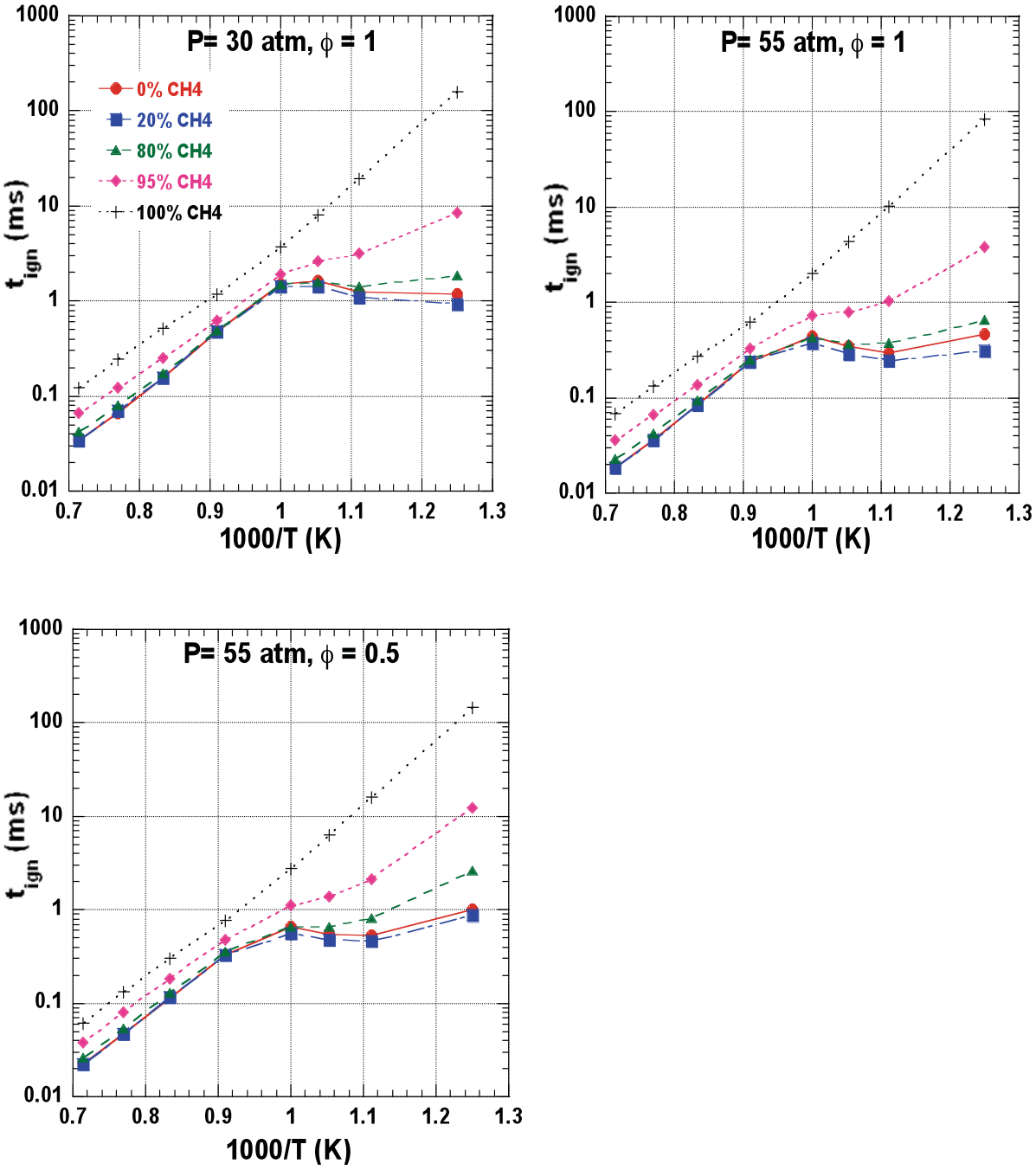

Figure 11: Predicted ignition delay time plotted versus the inverse of temperature for five different n-C_7H_{16}–CH_4 blends with 0% CH_4 (Circle), 20% CH_4 (Square), 80% CH_4 (Triangle), 95% CH_4 (Diamond) & 100% CH_4 (Cross Symbol). Other conditions are p=30 atm and ϕ=1 (Fig. a), p=55 atm and ϕ=1 (Fig. b), and p=55 atm and ϕ=0.5, (Fig. c).